Original Article

www.jmss.mui.ac.ir

Design and Fabrication of an Instrumented Handrim to Measure the Kinetic and Kinematic Information by the Hand of User for 3D Analysis of Manual Wheelchair Propulsion Dynamics

Mohammadreza Mallakzadeh, Hossein Akbari[1]

Department of Mechanical Engineering, Biomechanics Group, [1]Department of Mechanical Engineering, Production and Manufacturing Group - Mechatronics, Iran University of Science and Technology, Tehran, Iran

Submission: 04-10-2013 Accepted: 10-08-2014

ABSTRACT

The repetitious nature of propelling a wheelchair has been associated with the high incidence of injury among manual wheelchair users (MWUs), mainly in the shoulder, elbow and wrist. Recent literature has found a link between handrim biomechanics and risk of injury to the upper extremity. The valid measurement of three-dimensional net joint forces and torques, however, can lead to a better understanding of the mechanisms of injury, the development of prevention techniques, and the reduction of serious injuries to the joints. In this project, an instrumented wheel system was developed to measure the applied loads dynamically by the hand of the user and the angular position of the wheelchair user's hand on the handrim during the propulsion phase. The system is composed of an experimental six-axis load cell, and a wireless eight channel data logger mounted on a wheel hub. The angular position of the wheel is measured by an absolute magnetic encoder. The angular position of the wheelchair user's hand on the handrim during the propulsion phase (ϕ) or point of force application (PFA) is calculated by means of a new-experimental method using 36 pairs of infrared emitter/receiver diodes mounted around the handrim. In this regard, the observed data extracted from an inexperienced able-bodied subject pushed a wheelchair with the instrumented handrim are presented to show the output behavior of the instrumented handrim. The recorded forces and torques were in agreement with previously reported magnitudes. However, this paper can provide readers with some technical insights into possible solutions for measuring the manual wheelchair propulsion biomechanical data.

Key words: *Biomechanics, handrim, instrumented wheel system, kinetic and kinematic, manual wheelchairs, propulsion analysis, six-axis load cell*

INTRODUCTION

Wheelchair propulsion by manual wheelchair users (MWUs) has been described as the bilateral, simultaneous, repetitive motion of the upper extremities.[1] The repetitious nature of propelling a wheelchair has been associated with the high incidence of injury among MWUs.[2,3] In addition to the repetitiveness, high forces and awkward postures have been associated with injuries such as carpal tunnel syndrome (CTS), tendinitis, and shoulder rotator cuff injuries.[3-7] Although the shoulder is the most common site of musculoskeletal injury in MWUs, elbow, wrist, and hand pain, including CTS, are also commonly reported.[2,8-13] Sie *et al.*[13] have reported that elbow, wrist, and hand pain among MWUs are around 16, 13, and 11%, respectively. They defined significant pain as that which required analgesia and occurred with two or more activities of daily living or required the cessation of activity.[14] Using this definition, the prevalence of all upper extremity pain complaints was about 20% at 5 years postinjury and 46% at 15-19 years postinjury. Other studies have shown the prevalence of forearm, wrist, and hand pain to be between 8% and 55%, depending on the sample pool.[8,9] Recent literature has found a link between pushrim biomechanics and the risk of injury to the upper extremity.[15] In almost all of the studies on upper extremity pain, the authors felt that pain was related to overuse of the arm during transfers or wheelchair propulsion, and they have suggested that additional work aimed at prevention strategies is needed.[14]

The valid measurement of three-dimensional net joint forces and torques, however, can lead to a better understanding of

Address for correspondence:
Dr. Mohammadreza Mallakzadeh, Department of Mechanical Engineering, Iran University of Science and Technology, Zip Code: 16846-13114, Mail Box: 16765-163, Narmak, Tehran, Iran. E-mail: mmallak@iust.ac.ir

the mechanisms of injury, the development of prevention techniques, the reduction of serious injuries to the joints, and the explanation of the dynamics of wheelchair propulsion. The calculation of the net joint forces and torques that MWUs experience during manual wheelchair propulsion (MWP) requires the measurement of the loads acted onto the handrim. The complexity of developing a system for measuring handrim forces and torques has been reported in the literature.[14-18]

For a long time, there was no standard device to calculate the loads applied by the MWUs on the handrim, such as the force platform for gait analysis. Cooper *et al.*[16] have reported a few researchers have developed force-sensing systems and modeled wheelchair propulsion with varying degrees of success.[17-24] Rodgers *et al.*[25,26] have described an instrumented pushrim which was used in their studies at the Pennsylvania State University. Sixteen strain gauges were arranged in opposing pairs on each of four pushrim supports to form a single bridge. They have calculated peak and integral force variables. The mean force was determined from the integrated force divided by the mean contact time. Mean power was calculated from the mean force multiplied by the pushrim speed. They assumed that the point of force application (PFA) is coincident with a metacarpophalangeal (MCP) joint. Niesing *et al.*[27] have described a stationary ergometer. The ergometer allowed for the measurement of the propulsion torques around the wheel axle, the forces applied to the pushrims in three directions (tangential, radial, and axial) through transducers located in the wheel center. The ergometer was adjusted for each subject's anthropometric measurements. Torque curves of inexperienced subjects on the ergometer showed an initial negative deflection and a dip in the rising portion of the curve. This device was an important resource for the research program of the Faculty of Human Movement Sciences, VU University Amsterdam, and was used by van der Woude *et al.* and Veeger *et al.* in several studies.[28-34] Strauss *et al.*[35,36] have reported on the development of an instrumented wheel system (IWS). The calibration of their system revealed problems in terms of linearity and drift which only permitted reliable measurement of torque. A brief description of a second prototype was reported to employ an AMTI 6 degrees of freedom (DOF) force transducer. It was stated that their system transfers data from the sensor to a computer either through a direct wire link or via a microprocessor based digital FM transmitter-receiver system. Wu *et al.*[37] have performed static and dynamic analysis for their fabricated instrumented wheel using a commercial 6 DOF force transducer (JR-3 Inc., Woodland, CA). The system incorporates a data logger and a handrim unit mounted on a wheel hub. Excellent validity of the IWS is reported for both static and dynamic conditions on daily conventional wheelchairs. Brubaker *et al.*[38] examined the effect of horizontal and vertical seat position (relative to the wheel position) on the generation of static pushrim force. Force was measured using a test platform with a movable seat and strain gauged beams to which the pushrims were mounted. Pushing and pulling forces were recorded using a strip chart recorder. Brauer and Hertig[39] measured the static torque produced on push rims, which were rigidly restrained by springs and mounted independent of the tires and rims of the wheelchair. The spring system was adjustable to the subject's strength. The wheels were locked in a fixed position. Torque was measured using slide-wire resistors coupled to the differential movements between the pushrim and wheels and recorded using a strip chart recorder. Goosey-Tolfrey *et al.*[40] have developed an IWS to measure pushrim forces during racing wheelchair propulsion. Their system measured only two-dimensional forces and tangential and medial-lateral components. Mallakzadeh *et al.*[41-43] presented an IWS using a six-component load cell (Model PY6-500, Bertec Inc., Columbus, OH) that was fabricated and validated by using general uncertainty analysis. Furthermore, they determined the specifications of their IWS, the linearity, repeatability and the mean error by using both static and dynamic experiments. The results indicated that the uncertainty levels for the forces and moments of interest are in the range of 1.4-1.7 N and 0.58-0.68 N-m in the plane of the handrim, and about 3.40 N and 0.25 N-m in the wheel axle direction, respectively. Limroongreungrat *et al.*[44] presented an attempt to design and validate an IWS using a commercial force transducer (Model 45E15A-U760, JR-3, Inc., Woodland, CA) to measure three-dimensional pushrim forces of wheelchair propulsion in a racing wheelchair. Linearity, precision, and percent error were determined for both static and dynamic conditions. For the static condition, the IWS demonstrated a high linearity ($0.91 \leq$ slope ≤ 1.41) with $<2.72\%$ error rate. Under dynamic loading, the IWS provided the well-matched measurement forces with the predicted values from the inverse dynamics method ($0.96 \leq$ slope ≤ 1.07) with $<4.32\%$ error rate.

The SMART^{Wheel} is a pushrim force and torque sensor which is designed, fabricated, calibrated, and tested.[14-18,24,45-50] at the University of Pittsburgh through a pilot study and used for several researches. This system design is based on equations for a three-beam (120° apart) system for pushrim force and torque detection utilizing strain gauges. The last Clinical Version of SMART^{Wheel} calculates Push Forces, Push Frequency, Push Length, Push Smoothness and Speed. The system consists of a 2.4 GHz Wi-Fi 802.11b wireless access point that can be plugged into a standard ethernet network interface card, allowing a data collection range up to 300 ft indoors and 500 ft outdoors. The percent linearity for the moment and force were found to be 99.1% and 98.9%, respectively. They determined the uncertainty for the forces and moments as 1.1-2.5 N and 0.03- 0.19 N-m in the plane of the handrim, and 0.93 N and 2.24 N-m in the wheel axle direction, respectively.[50] This expensive IWS is now commercially available.

In this study, a new IWS is designed and fabricated to measure the three-dimensional handrim reaction loads applied by MWUs on the handrim, which are required for three-dimensional analysis of MWP dynamics. To measure three-dimensional forces and torques, an experimental six-axis load cell and a wireless eight channel data logger are mounted on a wheel. The specifications of the experimental six-axis load cell have been reported in the literature.[51] By developing the transformation equations, the actual forces and torques on the hand of the MWUs are calculated. The angular position of the wheel is measured by an absolute magnetic encoder. The angular position of the wheelchair user's hand on the handrim during the propulsion phase is calculated by means of a new experiment method using 36 pairs of infrared (IR) 3 mm emitter/receiver diodes that mounted around the handrim. The system is named hand-handrim positioning system (HHPS). Data from an inexperienced able-bodied subject pushed a wheelchair with the instrumented handrim showed patterns and overall behavior of instrumented handrim comparable to published data, and it has provided a temporal validation of the ability of IWS to detect forces and torques applied to the wheelchair handrim.

MATERIALS AND METHODS

To measure the forces and torques applied by MWUs on the handrim during MWP, we have conducted an experimental method to develop a new IWS. The device consists of three parts: Mechanical, electronic, and software.

Mechanical Part

The handrim assembly is attached to a 15 mm thick round plexiglas disc via four L-shaped slotted beams upon which various size handrims can be mounted. Besides, the distance between handrim and wheel is adjustable. The assembled handrim is mounted directly to the experimental six-axis load cell without connecting to other parts of the wheel. The other end of the load cell is attached to a round aluminum retainer that is mounted on a wheel hub. Therefore, when the handrim is grasped or struck and pushed downward and forward, in turn, rotating the wheels, the three-dimensional applied loads by MWUs pass the six-axis load cell, and we can detect them. The assembled IWS is presented in Figure 1.

Electronic Part

We developed the experimental six-axis load cell based on hollow cylindrical structure and six full strain gauge bridges. This transducer has a full mechanical loading rate of 200 N for in-plane axes (x and y), 3.5 KN for the out-plane axis (z), 80 N-m for moments M_x and M_y, and 120 N-m for moment M_z. Other specifications of the load cell have been reported in the literature.[51] The signal processing

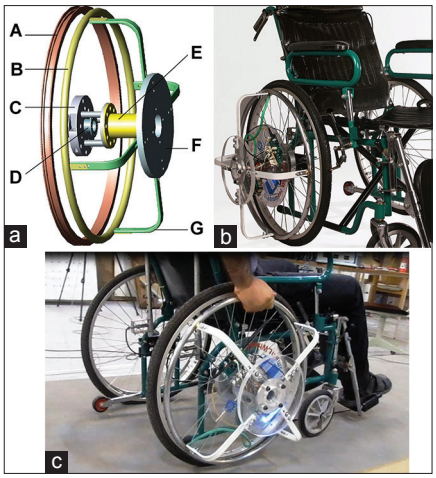

Figure 1: (a) The components of the instrumented wheel system (IWS). (A) wheel, (B) handrim, (C) retainer, (D) wheel hub, (E) experimental sis-axis load cell, (F) plexiglas disc, (G) L-shaped slotted beam. (b) The assembly of the IWS. (c) An inexperienced able-bodied subject pushed a wheelchair with the instrumented handrim

was implemented with a data logger that it is based on an 8/16-bit ATxmega32A4 Microcontroller from Atmel®.

The analog voltage signals coming from six channels of the load cell are converted to digital values in every 800 microseconds, utilizing three 24-bit AD7190 strain gauge signal conditioner chips,[52] one chip for each of two bridges. The AD7190 is a low noise, complete analog front end for high precision measurement applications. It contains a low noise, 24-bit sigma-delta ($\sum$-Δ) analog-to-digital converter. The AD7190 can be programmed to have a gain of 1, 8, 16, 32, 64, and 128. The excitation voltage is set to 5V dc using REF02 chip. The angular position of the wheel (α) is measured by an AS5045 chip.[53] The AS5045 is a contactless magnetic rotary encoder for accurate angular measurement over a full turn of 360°. To measure the angle, only a simple two-pole magnet, rotating over the center of the chip or vice versa, is required. Pulse width modulation (PWM) output of AS5045 provides a pulse width duty cycle that is proportional to the absolute angular position. PWM output is encoded in 12-bit resolutions. How the encoder was assembled is presented in Figure 2.

The signals of the six bridges, absolute encoder, and HHPS (8 channels total) were collected at 50 Hz with the ATxmega32A4. An nRF24L01 + was used to wirelessly and simultaneously transmit the signals of the six bridge, encoder, and HHPS of the wheel to the laptop. The nRF24L01 + is a single chip 2.4GHz transceiver with an embedded baseband protocol engine (Enhanced ShockBurst™), suitable for ultra-low power wireless applications. The nRF24L01 + is designed for operation in the worldwide ISM (industrial, scientific and medical) frequency band at 2.400-2.4835GHz. The printed circuit board is designed so that the analog and digital sections are separated. Furthermore, two push

buttons were used to zero angular position of the encoder and eliminate the offset of six channels of the load cell due to the error of the electrical components. All components are powered by a 12V 2000mAh Li-ion battery. It can be used for more than 3 h before recharging. Signals flow cycle of the instrumented handrim from date logger to laptop is showed in Figure 3.

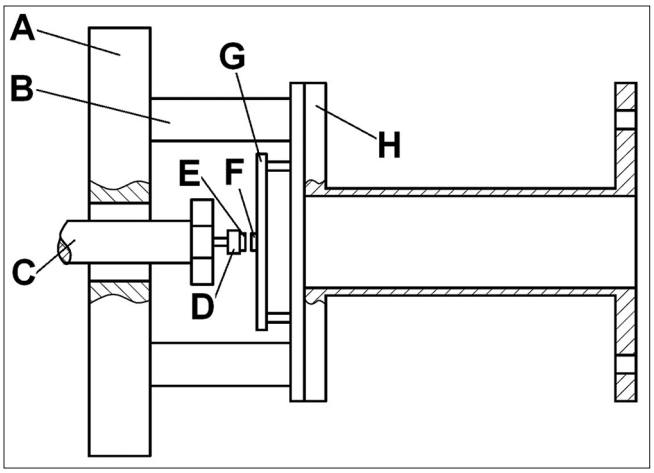

Figure 2: A layout represents how the encoder was assembled (A) retainer, (B) bush, (C) wheel axle, (D) allen screw, (E) magnet, (F) AS5045, (G) circuit board of AS5045, (H) load cell

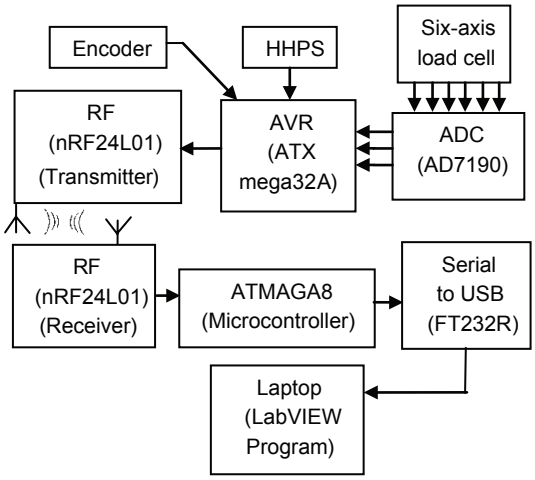

Figure 3: Signal flow cycle of the instrumented handrim

Software Part

The instrumented software was developed using LabVIEW 11.0.1 (2011).[54] The program converts channel data and position data to forces and torques, then stores the data on file.

Wheelchair

An FS902GC-46 reclining wheelchair with powder coating steel frame,[55] standard pushrims of 0.258 m radius, reclining high back, movable armrest, elevating footrest, solid castor, and pneumatic rear tires is used in this study. Furthermore, the position of the wheel axel is adjusted to the seat.

Mathematical Development

To characterize and measure the forces and torques applied by hand on the handrim we used three different coordinate systems. The global and the load cell coordinate systems have the same origin at the center of the wheel and the same directions at the beginning of the propulsion [Figure 4a].

The load cell coordinate system rotates with the wheel. The origin of the hand coordinate system is at the contact point between the hand and the handrim and moves with the handrim, but its axes remain parallel to the axes of the global coordinate system, [Figure 4b]. This is included in the next section.

Preloads

During the propulsion phase, in addition to the loads produced by the user's hand, the IWS experiences a dynamic offset due to the weight of the instrumented handrim which should be eliminated.

We pushed the wheelchair without applying any forces and torques on the instrumented handrim to measure the net preloads. As the preloads change sinusoidally with the rotation of the wheel, data were recorded and subtracted from the propulsion data with respect to the load cell

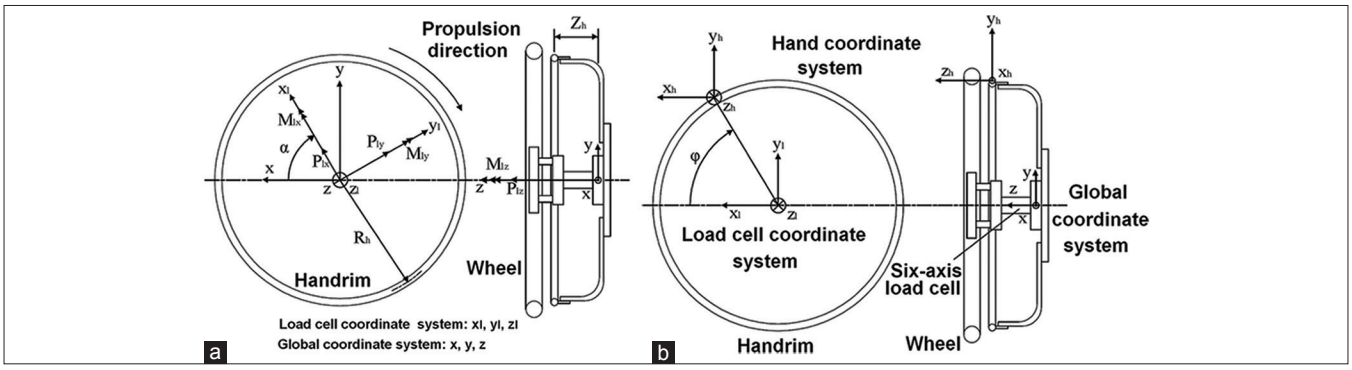

Figure 4: (a) Global and load cell coordinate systems. (b) Hand coordinate system on the handrim

coordinate system. As the wheel is rotated, the system records three-dimensional measurements of handrim loading at each 0.3° of the wheel angle. After the full turn of the wheel, the loads at each wheel angle, F_{px}, F_{py}, F_{pz}, M_{px}, M_{py}, and M_{pz} are saved on the Excel offset file, consisting of 1200 rows and 7 columns.

Load cell, global, and hand forces and torques

Forces and torques produced by the load cell are not providing the values required for the analysis. Data in the offset file is subtracted from all subsequent data before it is converted into handrim forces and torques. By using the following equations we calculate the net local forces and torques with respect to the load cell coordinate system.

$$F_{lx} = F_x - F_{px}$$

$$F_{ly} = F_y - F_{py}$$

$$F_{lz} = F_z - F_{pz}$$

$$M_{lx} = M_x - M_{px} \quad (1)$$

$$M_{ly} = M_y - M_{py}$$

$$M_{lz} = M_z - M_{pz}$$

where F_{lx}, F_{ly}, F_{lz}, M_{lx}, M_{ly}, and M_{lz} are the forces and torques applied by the wheelchair user, and F_x, F_y, F_z, M_x, M_y and M_z are the measured forces and torques. All values are with respect to the load cell coordinate system at the center of the wheel. The load cell coordinate system is fixed to the wheel and rotates with it.

Hence, we need to use the global coordinate system to calculate the forces and moments with respect to a reference system. Therefore, the next step is to transform the values from the load cell to the global coordinate system. We emphasize that the origin of the global coordinate system coincides with that of the transducer coordinate system, and their z axes are aligned. To obtain the forces and moments in the global coordinate system, we use the following transformation relations with reference to Figure 4b. α is wheel rotation angle that is measured with absolute encoder [Figures 2 and 4a].

$$F_{gx} = \cos\alpha \times F_{lx} - \sin\alpha \times F_{ly}$$

$$F_{gy} = \sin\alpha \times F_{lx} + \cos\alpha \times F_{ly}$$

$$F_{gz} = F_{lz} \quad (2)$$

$$M_{gx} = \cos\alpha \times M_{lx} - \sin\alpha \times M_{ly}$$

$$M_{gy} = \sin\alpha \times M_{lx} + \cos\alpha \times M_{ly}$$

$$M_{gz} = M_{lz}$$

These relations can be expressed in the matrix form as

$$\begin{bmatrix} F_{gx} \\ F_{gy} \\ F_{gz} \\ M_{gx} \\ M_{gy} \\ M_{gz} \end{bmatrix} = \begin{bmatrix} \cos(\alpha) & -\sin(\alpha) & 0 & 0 & 0 & 0 \\ \sin(\alpha) & \cos(\alpha) & 0 & 0 & 0 & 0 \\ 0 & 0 & 1 & 0 & 0 & 0 \\ 0 & 0 & 0 & \cos(\alpha) & -\sin(\alpha) & 0 \\ 0 & 0 & 0 & \sin(\alpha) & \cos(\alpha) & 0 \\ 0 & 0 & 0 & 0 & 0 & 1 \end{bmatrix} \begin{bmatrix} F_{lx} \\ F_{ly} \\ F_{l_z} \\ M_{lx} \\ M_{ly} \\ M_{lz} \end{bmatrix} \quad (3)$$

and in compact form as

$$\widehat{F}_g = T_l \cdot \widehat{F}_l \quad (4)$$

where T_l is the transformation matrix for transforming the load cell into global values, $\widehat{F}_g$ represents the vector of global forces and torques and $\widehat{F}_l$ is a vector of load cell forces and torques.

Since we need forces and torques at the contact point between the hand of the wheelchair user and the handrim during the pushing phase, we need another transformation from the global coordinate system to the hand coordinate system. The forces and torques in this coordinate system without camber or misalignment with reference to Figures 4b and 5 are as follows.

$$F_{hx} = F_{gx}$$

$$F_{hy} = F_{gy}$$

$$F_{hz} = F_{gz} \quad (5)$$

$$M_{hx} = M_{gx} - F_{gz} \times R_h \times \sin\varphi + F_{gy} \times Z_h$$

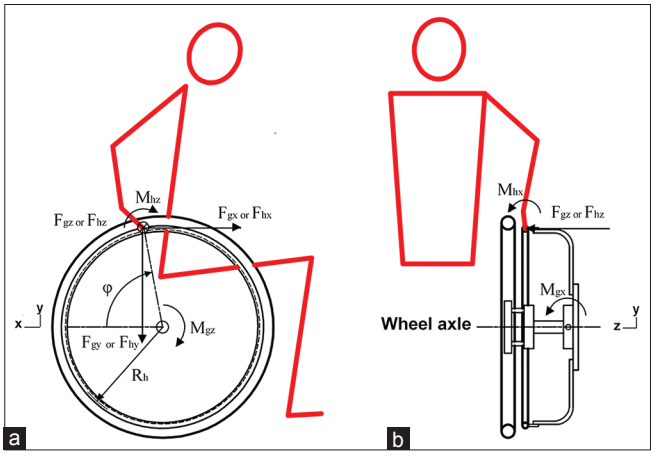

Figure 5: Illustration of forces and torques applied on the handrim. (a) Side view, (b) Back view

$$M_{hy} = M_{gy} + F_{gz} \times R_h \times \cos\varphi - F_{gx} \times Z_h$$

$$M_{hz} = M_{gz} + R_h \times \left(F_{gx} \times \sin\varphi - F_{gy} \times \cos\varphi\right)$$

where R_h is the handrim radius; and Z_h is the offset distance between the plane of handrim and the origin of the global coordinate system in the z direction. Furthermore, the angle φ is the instantaneous position of the hand on the handrim in the global coordinate system (x-y plane and $z = Z_h$) with respect to the + x-axis, and clockwise direction [Figure 4].

These relations can be expressed in the matrix form as

$$\begin{bmatrix} F_{hx} \\ F_{hy} \\ F_{hz} \\ M_{hx} \\ M_{hy} \\ M_{hz} \end{bmatrix} = \begin{bmatrix} 1 & 0 & 0 & 0 & 0 & 0 \\ 0 & 1 & 0 & 0 & 0 & 0 \\ 0 & 0 & 1 & 0 & 0 & 0 \\ 0 & Z_h & -R_h \sin\varphi & 1 & 0 & 0 \\ -Z_h & 0 & R_h \cos\varphi & 0 & 1 & 0 \\ R_h \sin\varphi & -R_h \cos\varphi & 0 & 0 & 0 & 1 \end{bmatrix} \begin{bmatrix} F_{gx} \\ F_{gy} \\ F_{gz} \\ M_{gx} \\ M_{gy} \\ M_{gz} \end{bmatrix} \quad (6)$$

and in a compact form as

$$\hat{F}_h = T_h \cdot \hat{F}_g \quad (7)$$

where T_h is the transformation matrix for transforming the global into hand values, $\hat{F}_g$ represents the vector of global forces and torques and $\hat{F}_h$ is the vector of hand forces and torques.

Determining the Position of the Hand on the Handrim

Forces and torques applied to the wheelchair handrim are generally recorded in a global x-y-z coordinate system. To obtain net joint force and torque estimations in hand coordinate system, a point that best represents the location where the loads are being applied must be identified. This point is called the PFA, and is similar to the center of pressure (COP) in gait studies.[14] In MWP, however, the MWUs grips the handrim, and therefore can potentially apply a moment about any of the coordinate axes. Hence, COP is a virtual PFA in three spaces, which accounts for the actual forces and torques measured at the wheel hub.[46] Several authors have extensively studied the calculation, both in two-dimensions and in three-dimensions, of the PFA using kinematic and kinetic data[14,16,25,31,46,51,57] Veeger *et al.* used φ to describe the PFA.[31] However, in their work it was defined to be coincident with an MCP joint. Rogers *et al.*[25,26] assumed that the PFA is coincident with an MCP joint. Cooper *et al.*[14] were the first authors to propose the use of PFA or COP to analyze MWP technique.

Traditionally, determining the location of the PFA in handrim wheelchair propulsion has been done through one of the two ways: (1) using kinematic data, assuming that the PFA is located at one of the MCP joints; or (2) using kinetic data, assuming that one or more of the handrim moment components applied are negligible and calculating the location of the PFA from loads data collected at the wheel hub.[56] All PFA values calculated with kinetic data were unstable at the beginning and end of the propulsion phase.[16] In fact, the location of the PFA can have an uncertainty of 100% at the beginning and end of the stroke cycle,[50] suggesting that it may be of limited use in some portions of the propulsion phase. Likewise, assuming that the PFA is located at the second MCP joint, leads to some minor inaccuracies in the computation of handrim force and torques components, but results in stable data throughout the propulsion phase.[56]

In this study, we have developed a new experiment system (HHPS) to approximate the position of the PFA tangent to the handrim. This system is equivalent to the kinematic method without the aid of an anatomical marker and camera system. In addition, an HHPS program was developed using LabVIEW. A flowchart of the HHPS program is showed in Figure 6.

In this method first, the angle ω_i is measured using 36 pairs of IR 3 mm LED emitter/receiver diodes mounted every 10° around the handrim [Figure 7]. The coupling diodes are labeled (i = 0 to 35). The ω_i of each coupling diode is determined relative to reference coupling diode (i = 0).

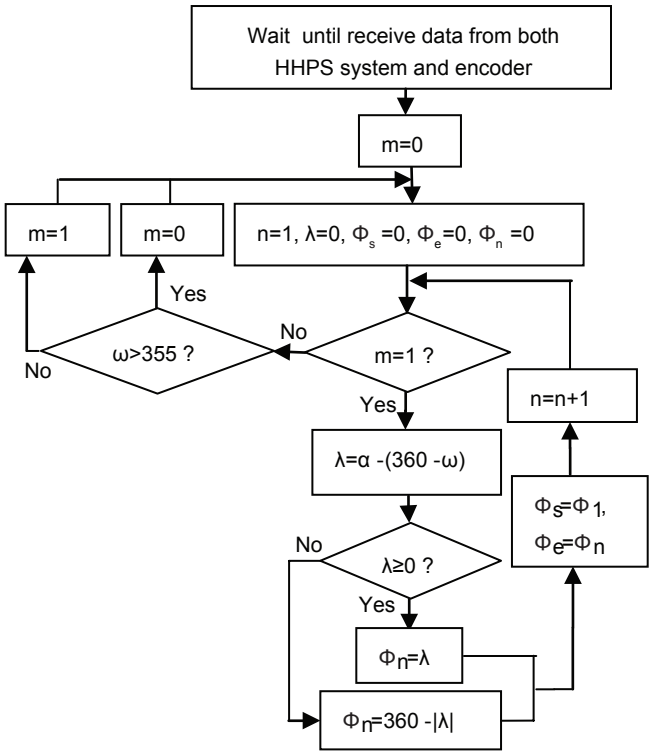

Figure 6: Flowchart of the hand-handrim positioning system program

When the hand grasps the handrim and covers n numbers of coupling diodes, ω is calculated as:

$$\omega = \frac{\sum_{i=0}^{35} \omega_i}{n} \quad (8)$$

φ_n is the instantaneous angle of the φ in the global coordinate system with respect to the + x-axis, and clockwise direction. Start angle (φ_s) is the angle between the line that is defined by the hand's first contact point on the handrim and the center of the wheel and the + x-axis. End angle (φ_e) is the angle between the line that is defined by the hand's last contact point on the handrim and the center of the wheel and the + x-axis [Figure 8].

Once the IWS is assembled, first + x-axis of the load cell and then the line that is defined by the reference coupling diode and the center of the wheel, are matched along + x-axis of global coordinate system using two push buttons.

RESULTS AND DISCUSSION

Using Equation (1-3), we calculated global forces and torques during the propulsion phase. The global forces are the same as the hand local forces. Figures 9 and 10 show the forces and torques produced by the wheelchair user during the pushing phase on the handrim with respect to the global coordinate system. The figure shows a spike on the curve for F_{gy}, F_{gz}, M_{gx}, M_{gz} during the first time of the propulsion phase. This spike appears in our results because we used an able-bodied subject (inexperienced wheelchair user) [Figure 1c].

The φ_s, φ_e, and the contact angle (φ_c) during five revolution of the wheel calculated using the HHSP system are presented in Table 1.

Besides, Figure 11 shows the time variation of φ at different angle of α for two strokes. Figure 12 shows the torques produced by the wheelchair user hand with respect to the hand coordinate system. These torques were calculated through equation (5).

Table 1: Angular position of the hand on the handrim during five propulsion phase

Stroke	φ_s	φ_e	φ_c
1	74	149.7	75.7
2	75.2	140.8	65.6
3	73.2	152.9	79.7
4	85.7	164.1	78.4
5	60.9	141.4	80.5

φ_s – Start angle; φ_e – End angle; φ_c – Contact angle

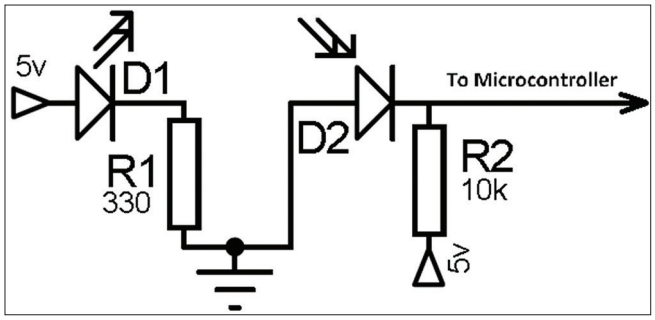

Figure 7: Circuit diagram for coupling diode, D1 is emitter diode, D2 is receiver diode

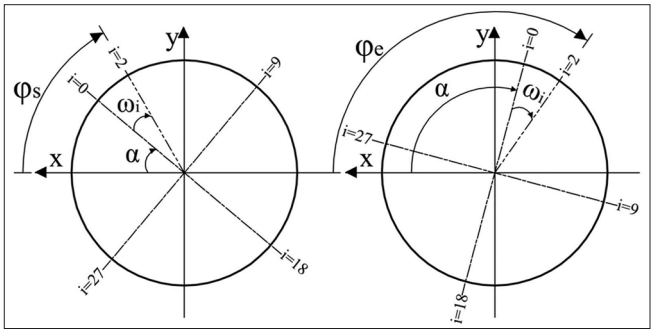

Figure 8: The angles α, wi, φs, φe for a complete stroke cycle of the manual wheelchair propulsion

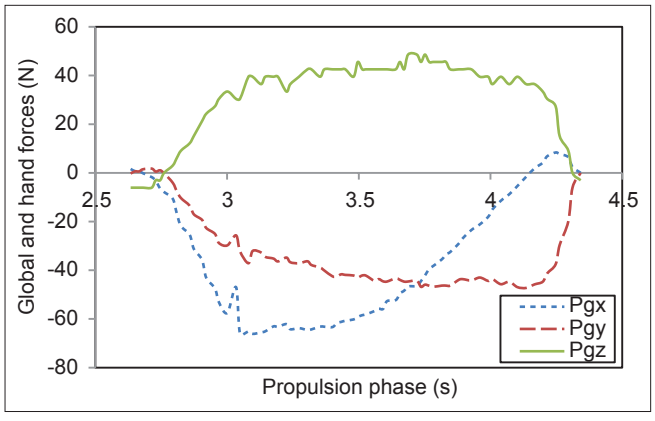

Figure 9: Propulsion force components with respect to global and hand coordinate systems

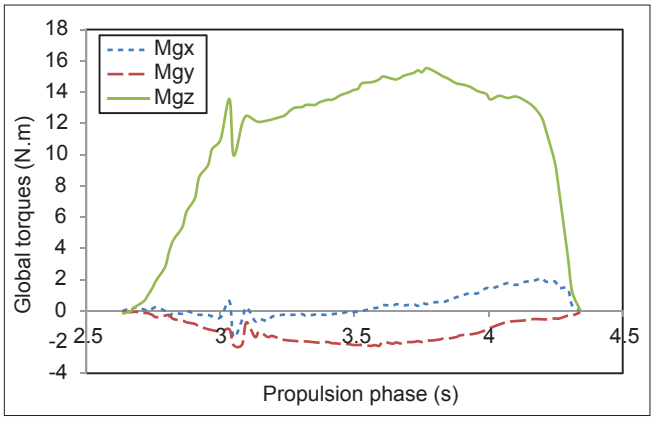

Figure 10: Propulsion torque components with respect to global coordinate system

Using hand force components (F_{hx}, F_{hy}, and F_{hz}) produced by the able-bodied subject, we obtained the total force (F_{total}) applied on the handrim, equation (9). The total effective force (TEF), which is a virtual force in order to produce propulsion, is obtained by expressing it in terms of M_{gz}, the moment around the z-axis and the handrim radius, equation (10). The fractional effective force (FEF) is an important factor because it shows the ratio of the required force for propulsion and the force produced by the wheelchair user during the propulsion phase, equation (11). FEF (in percentage) is related to F_{total} and TEF as in equation (11).[33,42,58,59]

$$F_{total} = \sqrt{\left(F_{hx}^2 + F_{hy}^2 + F_{hz}^2\right)} \quad (9)$$

$$TEF = M_{gz} \cdot R_h^{-1} \quad (10)$$

$$FEF = \left(TEF / F_{total}\right) \times 100 \quad (11)$$

Figure 13 shows the total force and TEF which are calculated using the equation (9 and 10) and the data from the main test.

Considering the generally low level of efficiency for MWP, it is reasonable to expect a lower value for the TEF compared with the total force produced during the propulsion phase. To improve the MWP, we should attempt to decrease the value of the total force as much as possible, closer to the value of the TEF by choosing proper wheelchair size, and seating position for each user.[42]

The FEF is an important factor, which is used as an alternative to efficiency to verify how effective the MWP is.[42]

Figure 14 shows that FEF has lower values at approximately first 10% and the last 15% of the propulsion phase. We do not have high reliability at the first and the last 10% of the propulsion phase because of the vibrations due to the initial contact between the hand and the handrim and releasing the handrim.

CONCLUSION

The valid measurement of three-dimensional net joint forces and torques can lead to the reduction of injuries of the upper extremity for MWUs. A reliable IWS can measure the magnitude of the forces and torques exerted on the handrim by the MWUs, from which the variation and sensitivity of the other important parameters, such as the TEF and the FEF, can be determined. This study was

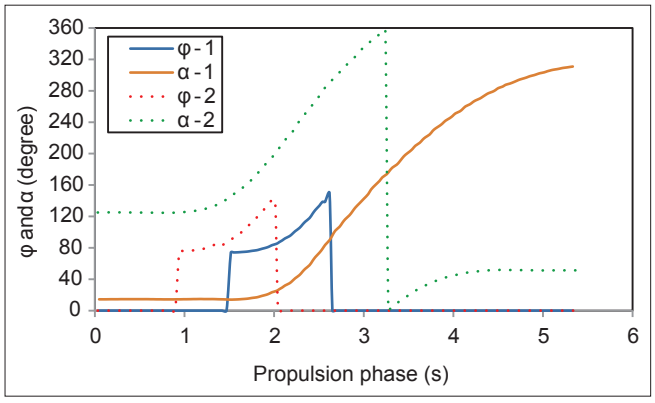

Figure 11: Angular position of the hand on the handrim (φ) and wheel rotation angle (α) with respect to global coordinate system for two strokes

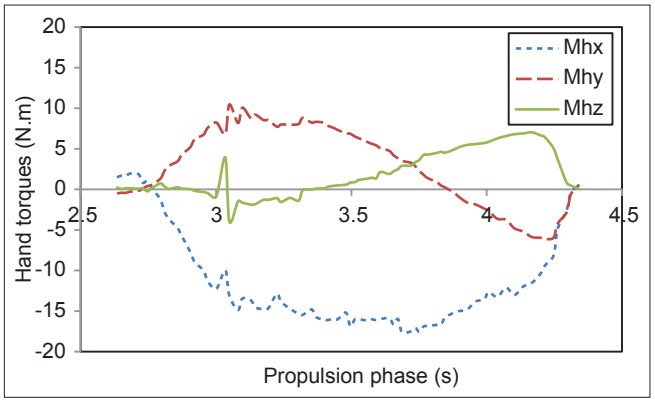

Figure 12: Propulsion torque components with respect to hand coordinate system

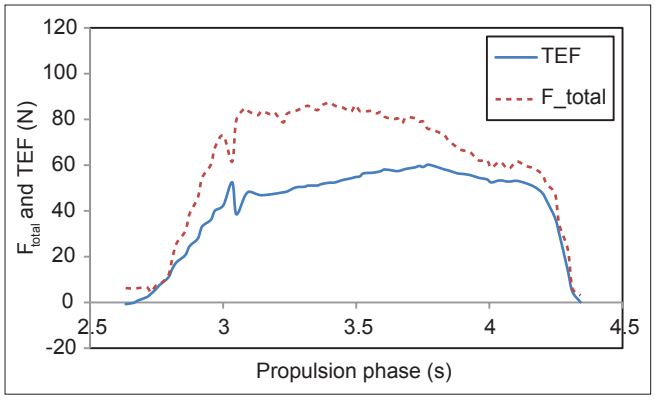

Figure 13: The total force (F_{total}) and the total effective force

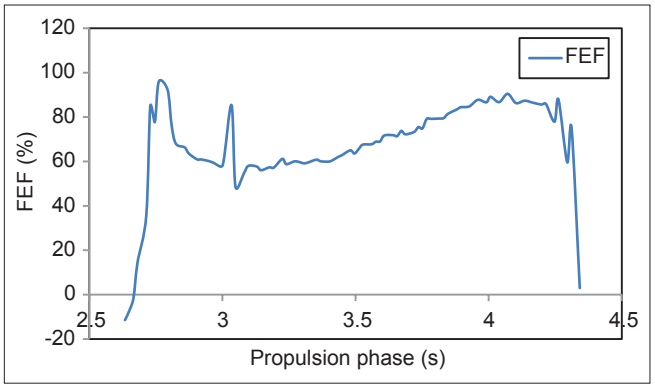

Figure 14: The fractional effective force during the propulsion phase

performed to develop an IWS for kinetic and kinematic measurement of MWP information, which is required for three-dimensional analysis of MWP dynamics. The applied forces and torques between the wheelchair user's hand and the handrim were measured at the wheel hub using an experimental six-axis load cell. The angular position of the hand on the handrim during the pushing phase (φ) was calculated by developing a new system without using cameras or motion analysis system. Using a camera system, the hand angular position during the propulsion phase can be validated. Microsoft® Excel® 2007 (12.0.4518.1014) and LabVIEW™ 2011 (11.0.1) software are used to calculate all loads and φ. The transformation matrix between the local and global loads has been determined, and the applied forces and torques between the wheelchair user's hand and the handrim were calculated. The tests with an able-bodied subject reproduced patterns and overall behavior comparable to the available data indicates that the system can be used for designed and planned experiments. Further studies are needed to determine the specifications of the IWS by performing static and dynamic verification tests.

Nomenclature

F_x (N)	The force along the X-axis in the load cell coordinate system
F_y (N)	The force along the Y-axis in the load cell coordinate system
F_z (N)	The force along the Z-axis in the load cell coordinate system
M_x (N.m)	The torque about the X-axis in the load cell coordinate system
M_y (N.m)	The torque about the Y-axis in the load cell coordinate system
M_z (N.m)	The torque about the Z-axis in the load cell coordinate system
F_{px} (N)	The preload force along the X-axis measured without applying any load on the instrumented handrim in full turn of the wheel in the load cell coordinate system
F_{py} (N)	The preload force along the Y-axis measured without applying any load on the instrumented handrim in full turn of the wheel in the load cell coordinate system
F_{pz} (N)	The preload force along the Z-axis measured without applying any load on the instrumented handrim in full turn of the wheel in the load cell coordinate system
M_{px} (N.m)	The preload torque about the X-axis measured without applying any load on the instrumented handrim in full turn of the wheel in the load cell coordinate system
M_{py} (N.m)	The preload torque about the Y-axis measured without applying any load on the instrumented handrim in full turn of the wheel in the load cell coordinate system
M_{pz} (N.m)	The preload torque about the Z-axis measured without applying any load on the instrumented handrim in full turn of the wheel in the load cell coordinate system
F_{lx} (N)	The local force along the X-axis applied by the wheelchair user on the handrim in the load cell coordinate system
F_{ly} (N)	The local force along the Y-axis applied by the wheelchair user on the handrim in the load cell coordinate system
F_{lz} (N)	The local force along the Z-axis applied by the wheelchair user on the handrim in the load cell coordinate system

Contd...

Nomenclature

F_{lz} (N)	The local force along the Z-axis applied by the wheelchair user on the handrim in the load cell coordinate system
M_{lx} (N.m)	The local torque about the X-axis applied by the wheelchair user on the handrim in the load cell coordinate system
M_{ly} (N.m)	The local torque about the Y-axis applied by the wheelchair user on the handrim in the load cell coordinate system
M_{lz} (N.m)	The local torque about the Z-axis applied by the wheelchair user on the handrim in the load cell coordinate system
F_{gx} (N)	The global force along the X-axis applied by the wheelchair user on the handrim in the global coordinate system
F_{gy} (N)	The global force along the Y-axis applied by the wheelchair user on the handrim in the global coordinate system
F_{gz} (N)	The global force along the Z-axis applied by the wheelchair user on the handrim in the global coordinate system
M_{gx} (N.m)	The global torque about the X-axis applied by the wheelchair user on the handrim in the global coordinate system
M_{gy} (N.m)	The global torque about the Y-axis applied by the wheelchair user on the handrim in the global coordinate system
M_{gz} (N.m)	The global torque about the Z-axis applied by the wheelchair user on the handrim in the global coordinate system
F_{hx} (N)	The hand force along the X-axis applied by the wheelchair user on the handrim in the hand coordinate system
F_{hy} (N)	The hand force along the Y-axis applied by the wheelchair user on the handrim in the hand coordinate system
F_{hz} (N)	The hand force along the Z-axis applied by the wheelchair user on the handrim in the hand coordinate system
M_{hx} (N.m)	The hand torque about the X-axis applied by the wheelchair user on the handrim in the hand coordinate system
M_{hy} (N.m)	The hand torque about the Y-axis applied by the wheelchair user on the handrim in the hand coordinate system
M_{hz} (N.m)	The hand torque about the Z-axis applied by the wheelchair user on the handrim in the hand coordinate system
F_{total} (N)	The total force applied on the handrim in the hand coordinate system
TEF (N)	The total effective force which is a virtual force in order to produce propulsion
FEF (in percentage)	The fractional effective force is a factor which shows the ratio of the required force for propulsion and the force produced by the wheelchair user during the propulsion phase
α (deg)	The wheel rotation angle
φ (deg)	The instantaneous position angle of the hand on the handrim
φ_s (deg)	The start angle of φ
φ_e (deg)	The end angle of φ
φ_c (deg)	The contact angle
ωi (deg)	The angle of the coupling diodes are labeled (i=0-35) to reference coupling diode (i=0) on the handrim
Rh (m)	The handrim radius
Zh (m)	The offset distance between the plane of the handrim and the origin of the global coordinate system in the z direction

TEF – Total effective force; FEF – Fractional effective force

ACKNOWLEDGMENTS

The authors wish to thank Behzad Kadkhodaie for assistance with data collection.

REFERENCES

1. Davis R, Ferrara M. The competitive wheelchair stroke. Natl Strength Cond Assoc 1988;10:4-10.
2. Gellman H, Chandler DR, Petrasek J, Sie I, Adkins R, Waters RL. Carpal tunnel syndrome in paraplegic patients. J Bone Joint Surg Am 1988;70:517-9.
3. Apple DF, Cody R, Allen A. Overuse syndrome of the upper limb in people with spinal cord injury. In: Physical Fitness: A Guide for Individuals with Spinal Cord Injury. Journal of Rehabilitation Research and Development, Chapter 5, 1996, 97-108.
4. Armstrong TJ, Fine LJ, Goldstein SA, Lifshitz YR, Silverstein BA. Ergonomics considerations in hand and wrist tendinitis. J Hand Surg Am 1987;12:830-7.
5. Silverstein BA, Fine LJ, Armstrong TJ. Occupational factors and carpal tunnel syndrome. Am J Ind Med 1987;11:343-58.
6. Silverstein BA, Fine LJ, Stetson D. Hand-wrist disorders among investment casting plant workers. Hand Surg 1987;12A: 838-44.
7. Silverstein BA, Fine LJ, Armstrong TJ. Hand wrist cumulative trauma disorders in industry. Br J Ind Med 1986;43:779-84.
8. Pentland WE, Twomey LT. The weight-bearing upper extremity in women with long term paraplegia. Paraplegia 1991;29:521-30.
9. Gellman H, Sie I, Waters RL. Late complications of the weight-bearing upper extremity in the paraplegic patient. Clin Orthop Relat Res 1988;233:132-5.
10. Bayley JC, Cochran TP, Sledge CB. The weight-bearing shoulder. The impingement syndrome in paraplegics. J Bone Joint Surg Am 1987;69:676-8.
11. Wylie EJ, Chakera TM. Degenerative joint abnormalities in patients with paraplegia of duration greater than 20 years. Paraplegia 1988;26:101-6.
12. Nichols PJ, Norman PA, Ennis JR. Wheelchair user's shoulder? Shoulder pain in patients with spinal cord lesions. Scand J Rehabil Med 1979;11:29-32.
13. Sie IH, Waters RL, Adkins RH, Gellman H. Upper extremity pain in the postrehabilitation spinal cord injured patient. Arch Phys Med Rehabil 1992;73:44-8.
14. Cooper RA, VanSickle DP, Robertson RN, Boninger ML, Ensinger GJ. A method for analyzing center of pressure during manual wheelchair propulsion. IEEE Trans Rehabil Eng 1995;3:289-98.
15. Boninger ML, Cooper RA, Baldwin MA, Shimada SD, Koontz A. Wheelchair pushrim kinetics: Body weight and median nerve function. Arch Phys Med Rehabil 1999;80:910-5.
16. Cooper RA, Robertson RN, VanSickle DP, Boninger ML, Shimada SD. Methods for determining three-dimensional wheelchair pushrim forces and moments: A technical note. J Rehabil Res Dev 1997;34:162-70.
17. Asato KT, Cooper RA, Robertson RN, Ster JF. SMARTWheels: Development and testing of a system for measuring manual wheelchair propulsion dynamics. IEEE Trans Biomed Eng 1993;40:1320-4.
18. VanSickle DP, Cooper RA, Robertson RN. SMART^{wheel}: Development of a digital force and moment sensing pushrim. In: Proceedings of the 18th International RESNA Conference, Vancouver, BC, Canada. Washington, DC: RESNA Press; 1995. p. 352-4.
19. Cooper RA. An exploratory study of racing wheelchair propulsion dynamics. Adapt Phys Act Q 1990:7:74-85.
20. Cooper RA. A force/energy optimization model for wheelchair athletics. IEEE Trans Syst Man Cybern 1990;20:444-9.
21. Cooper RA. A systems approach to the modeling of racing wheelchair propulsion. J Rehabil Res Dev 1990;27:151-62.
22. Gehlsen G, Bahamonde R. Shoulder joint forces and torques in wheelchair propulsion. In: Proceedings of the North American Congress on Biomechanics (NACOB) II, Chicago, USA; 1992. p. 459-60.
23. Su FC, Lin LT, Wu HW, Chou YL, Westreich A, An KA. Three-dimensional dynamic analysis of wheelchair propulsion. Chin J Med Biol Eng 1993;13:326-42.
24. Cooper RA, Cheda A. Measurement of racing wheelchair propulsion torque. In: Proceedings of IEEE-EMBS 11th International Conference. Vol. 11. 1989. p. 530-1531.
25. Rodgers MM, Tummarakota S, Lieh J, Schrag DR. Three-dimensional dynamic analysis of joint reaction forces and moments during wheelchair propulsion. In: Proceedings of the North American Congress on Biomechanics (NACOB) II, Chicago, USA; 1992. p. 457-8.
26. Rodgers MM, Gayle GW, Figoni SF, Kobayashi M, Lieh J, Glaser RM. Biomechanics of wheelchair propulsion during fatigue. Arch Phys Med Rehabil 1994;75:85-93.
27. Niesing R, Eijskoot F, Kranse R, den Ouden AH, Storm J, Veeger HE, *et al.* Computer-controlled wheelchair ergometer. Med Biol Eng Comput 1990;28:329-38.
28. van der Woude LH, Veeger HE, Rozendal RH. Propulsion technique in hand rim wheelchair ambulation. J Med Eng Technol 1989;13:136-41.
29. van der Woude LH, Janssen TW, Meijs PJ, Veeger HE, Rozendal RH. Physical stress and strain in active wheelchair propulsion: Overview of a research programme. Rehabil Sci 1994;7:18-25.
30. Veeger HE, van der Woude LH, Rozendal RH. Wheelchair propulsion technique at different speeds. Scand J Rehabil Med 1989;21:197-203.
31. Veeger HE, van der Woude LH, Rozendal RH. Load on the upper extremity in manual wheelchair propulsion. J Electromyogr Kinesiol 1991;1:270-80.
32. Veeger HE, van der Woude LH, Rozendal RH. Within-cycle characteristics of the wheelchair push in sprinting on a wheelchair ergometer. Med Sci Sports Exerc 1991;23:264-71.
33. Veeger HE, Lute EM, Roeleveld K, van der Woude LH. Differences in performance between trained and untrained subjects during a 30-s sprint test in a wheelchair ergometer. Eur J Appl Physiol Occup Physiol 1992;64:158-64.
34. Veeger HE, van der Woude LH, Rozendal RH. A computerized wheelchair ergometer. Results of a comparison study. Scand J Rehabil Med 1992;24:17-23.
35. Strauss MG, Moeinzadeh MH, Schneller M, Trimble J. The development of an instrumented wheel to determine the handrim forces during wheelchair propulsion. In: Proceedings of the American Society of Mechanical Engineers (ASME) Winter Annual Meeting; 1989. p. 53-4.
36. Strauss MG, Maloney J, Ngo F, Phillips M. Measurement of the dynamic forces during manual wheelchair propulsion. In: Proceedings of the 15th Annual Meeting of the American Society of Biomechanics; 1991. p. 210-1.
37. Wu HW, Berglund LJ, Su FC, Yu B, Westreich A, Kim KJ, *et al.* An instrumented wheel for kinetic analysis of wheelchair propulsion. J Biomech Eng 1998;120:533-5.
38. Brubaker CE, Ross S, McLaurin CA. Effect of seat position on handrim force. In: Proceedings of 5th Annual Conference Rehabilitation Engineering; 1982. p. 111.
39. Brauer RL, Hertig BA. Torque generation on wheelchair handrims. In: Proceedings of Biomechanics Symposium, ASMEIASCE Mechanics Conference; 1981. p. 113-6.
40. Goosey-Tolfrey VL, Fowler NE, Campbell IG, Iwnicki SD. A kinetic analysis of trained wheelchair racers during two speeds of propulsion. Med Eng Phys 2001;23:259-66.
41. Mallakzadeh MR, Sassani F, and Oxland T. Development of an instrumented wheel for three-dimensional analysis of manual wheelchair propulsion dynamics. In: Proceedings of International Symposium on Collaborative Research in Applied Science (ISOCRIAS),

Vancouver, Canada; 2005. p. 22-9.
42. Mallakzadeh M, Sassani F. An experimental technique to verify an instrumented wheelchair. Exp Tech 2007;31:25-33.
43. Mallakzadeh M, Sassani F. General uncertainty analysis for manual wheelchair propulsion dynamic and development of an instrumented wheel. ASME J Med Device 2007;1:140-50.
44. Limroongreungrat W, Wang YT, Chang L, Geil MJ, Johnson JY. Technical note: An instrumented wheel system for measuring 3-D pushrim kinetics during racing wheelchair propulsion. Int J Res Sports Med 2009;17:182-94.
45. Watanabe KT, Cooper RA, Ster JF. A device for studying wheelchair propulsion dynamics. In: Proceedings of the 13th International Conference of the IEEE Engineering in Medicine and Biology Society, Orlando, FL; 1991. p. 1817-8.
46. Cooper RA, Robertson RN, VanSickle DP, Boninger ML, Shimada SD. Projection of the point of force application onto a palmar plane of the hand during wheelchair propulsion. IEEE Trans Rehabil Eng 1996;4:133-42.
47. Cooper RA, DiGiovine CP, Boninger ML, Shimada SD, Robertson RN. Frequency analysis of 3-dimensional pushrim forces and moments for manual wheelchair propulsion. Automedica 1998;16:355-65.
48. Cooper RA, Asato KT, Robertson RN, Ster JF. 2-dimensional kinetic analysis of manual wheelchair propulsion with an improved SMART^{wheel}. In: Proceedings of the 14th International Conference of the IEEE Engineering in Medicine and Biology Society, Paris, France. Vol. 14, No. 4. 1992. p. 1544-5.
49. Robertson RN, Cooper RA. Kinetic characteristics of wheelchair propulsion utilizing the SMART^{wheel}. In: Proceedings of the 17th Annual Meeting of the American Society of Biomechanics, Iowa City, IA; 1993. p. 202-3.
50. Cooper RA, Boninger ML, VanSickle DP, Robertson RN, Shimada SD. Uncertainty analysis for wheelchair propulsion dynamics. IEEE Trans Rehabil Eng 1997;5:130-9.
51. Akbari. H, Mallakzadeh. M, Kadkhodaie. B. A six axis load cell with a wireless eight channel data logger, Iran. Patent, Pat. No. 80048, 2013.
52. Analog Devices, Inc., Norwood, Massachusetts, USA. Available from: http://www.analog.com (Retrieved: 10-08-2014).
53. Ams AG, Inc., Unterpremstätten, Austria. Available from: http://www.ams.com/eng (Retrieved: 10-08-2014).
54. LabVIEW 11.0.1 (2011), National Instruments Corporation, Austin, Texas, USA. Available from: http://www.ni.com/labview (Retrieved: 10-08-2014).
55. Guangzhou TOPMEDI Healthcare Co., Ltd., Guangdong, China. Available from: http://www.topmedi.com/en/index.asp (Retrieved: 10-08-2014).
56. Sabick MB, Zhao KD, An KN. A comparison of methods to compute the point of force application in handrim wheelchair propulsion: A technical note. J Rehabil Res Dev 2001;38:57-68.
57. VanSickle DP, Cooper RA, Boninger ML, Robertson RN, Shimada SD. A unified method for calculating the center of pressure during wheelchair propulsion. Ann Biomed Eng 1998;26:328-36.
58. Cooper RA, Boninger ML, VanSickle DP, DiGiovine CP. Instrumentation for measuring wheelchair propulsion biomechanics. In: Van der Woude LH, Hopman MT, van Kemenade CH, editors. Biomedical Aspects of Manual Wheelchair Propulsion. Amsterdam, The Netherlands: IOS Press; 1999. p. 104-14.
59. van Kemenade CH, Te Kulve KL, Dallmeije AJ, van der Woude LH, Veeger HE. Changes in wheelchair propulsion technique during rehabilitation. In: Van der Woude LH, Hopman MT, van Kemenade CH, editors. Biomedical Aspects of Manual Wheelchair Propulsion. Amsterdam, The Netherlands: IOS Press; 1999. p. 104-14.

How to cite this article: Mallakzadeh M, Akbari H. Design and Fabrication of an Instrumented Handrim to Measure the Kinetic and Kinematic Information by the Hand of User for 3D Analysis of Manual Wheelchair Propulsion Dynamics. J Med Sign Sence 2014;4:256-66.

Source of Support: Nil, **Conflict of Interest:** None declared

BIOGRAPHIES

Mohammadreza Mallakzadeh received his B.S. degree in Mechanical Engineering from Sharif University of Technology, Tehran, Iran, in 1992, the M.Sc. degree in Mechanical Engineering-Biomechanics from Sharif University of Technology, Tehran, Iran, in 1995, the Ph.D. degree in Mechanical Engineering-Biomechanics from The University of British Columbia, Vancouver, Canada in 2007. Since 1995 till 2002, he was an instructor at Iran University of Science and Technology (IUST) and from 2007 he has been a faculty member at IUST, in Tehran, Iran. Currently, he is an Assistant Professor of Biomechanics at School of Mechanical Engineering, IUST. His research interests are Rehabilitation, Injury Biomechanics and Sport Biomechanics.

E-mail: mmallak@iust.ac.ir

Hossein Akbari received his M.Sc. degree in Mechanical Engineering, from Iran University of Science and Technology, Tehran, Iran in 2013. Most of his research is on designing and fabricating of various mechatronics devices.

E-mail: hosein.akbarii@gmail.com